MOLECULAR IMAGING AND BIOLOGY

Mol Imaging Biol (2013) 15:534–541
DOI: 10.1007/s11307-013-0630-2

Published Online: 29 March 2013

World Molecular Imaging Society

RESEARCH ARTICLE

Feasibility of Lactadherin-Bearing Clinically Available Microbubbles as Ultrasound Contrast Agent for Angiogenesis

Kentaro Otani, Kenichi Yamahara

Department of Regenerative Medicine and Tissue Engineering, National Cerebral and Cardiovascular Center Research Institute, 5-7-1 Fujishiro-dai, Suita, Osaka 565-8565, Japan

Abstract

Objectives: Phagocytosis of apoptotic cells is carried out through bridging of phosphatidylserine (PS)-expressing apoptotic cells and integrin αvβ3-expressing phagocytes with lactadherin. The objective of this study was to examine whether microbubbles targeted to integrin αvβ3 could be produced by conjugating a PS-containing clinically available ultrasound contrast agent with lactadherin.

Materials and Methods: PS-containing perfluorobutane-filled microbubbles were incubated with R-phycoerythrin (PE)-labeled lactadherin, and the presence of PE-positive bubbles was examined by FACS analysis. Secondly, the attachment of lactadherin to integrin αvβ3-expressing cells (human umbilical vein endothelial cells (HUVEC)) was also examined by FACS analysis. Finally, the adhesion of PS-containing bubbles to HUVEC was examined using a parallel plate flow chamber. The number of adherent bubbles with or without the intermediation of lactadherin was compared.

Results: The more lactadherin was added to the bubble suspension, the more PE-positive bubbles were detected. The size of bubbles was not increased even after conjugation with lactadherin (2.90±0.04 vs. 2.81±0.02 μm). Binding between lactadherin and HUVEC was also confirmed by FACS analysis. The parallel plate flow chamber study revealed that the number of PS-containing bubbles adherent to HUVEC was increased about five times by the intermediation of lactadherin (12.1±6.0 to 58.7±33.1 bubbles).

Conclusion: Because integrin αvβ3 is well-known to play a key role in angiogenesis, the complex of PS-containing bubbles and lactadherin has feasibility as a clinically translatable targeted ultrasound contrast agent for angiogenesis.

Key words: Microbubble, Ultrasound molecular imaging, Sonazoid, Integrin αvβ3, Angiogenesis

Introduction

Ultrasound molecular imaging, which utilizes molecular-targeted bubbles, is a powerful tool for the noninvasive understanding of molecular dynamics *in situ*. The usefulness of ultrasound molecular imaging has been demonstrated in animal models of vascular disease and angiogenesis [1–4]. Although a lot of molecular-targeted bubbles have been developed for animal studies, the clinical translation of these targeted bubbles is still challenging.

Sonazoid (Daiichi-Sankyo Pharmaceuticals, Tokyo, Japan), perfluorobutane gas microbubbles stabilized by a membrane of hydrogenated egg phosphatidylserine (PS), is clinically available in Japan [5]. In 2000, Lindner et al. reported that PS-

Electronic supplementary material The online version of this article (doi:10.1007/s11307-013-0630-2) contains supplementary material, which is available to authorized users.

Correspondence to: Kentaro Otani; *e-mail:* otani@ri.ncvc.go.jp

containing bubbles could be labeled with annexin V [6]. Based on their result, we recently demonstrated the feasibility of preparation of antibody-carrying bubbles based on Sonazoid through annexin V and biotin-avidin complex formation [7]. Because annexin V binds with PS in a Ca^{2+}-dependent manner, the conjugation of antibodies was performed in the presence of Ca^{2+}. However, significant aggregation and disappearance of Sonazoid bubbles were observed after the addition of Ca^{2+} [7]. Additionally, the binding between Sonazoid bubbles and annexin V was quite fragile [7, 8]. Therefore, an alternative molecule that does not require Ca^{2+} for the detection of PS in Sonazoid is desirable in the preparation of targeted bubbles based on Sonazoid.

Milk fat globule epidermal growth factor 8 (MFG-E8)/lactadherin is a secreted glycoprotein which was originally identified as a component of milk fat globules [9]. Lactadherin contains a PS-binding C-domain and an RGD (arginine–glycine–aspartic acid) motif residing in the epidermal growth factor domain and has the feature of forming a bridge between PS on apoptotic cells and integrin αvβ3 on phagocytes [10–12]. It is noteworthy that the binding between PS and lactadherin is Ca^{2+}-independent [13, 14]. Therefore, we hypothesized that lactadherin has the potential to be a mediator between PS-containing bubbles and integrin αvβ3-expressing cells. In other words, the complex of PS-containing bubbles and lactadherin has the potential to be a novel integrin αvβ3-targeted ultrasound contrast agent (Fig. 1). The aim of this study was to examine whether microbubbles targeted to integrin αvβ3 could be produced by conjugating a PS-containing clinically available ultrasound contrast agent with lactadherin.

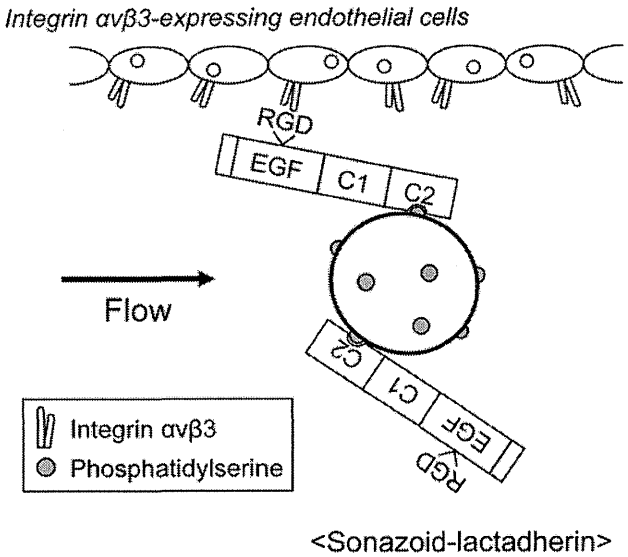

Fig. 1. Expected interaction between lactadherin-bearing Sonazoid bubbles and integrin αvβ3-expressing endothelial cells under flow condition. Epidermal growth factor-like domain (*EGF*), factor VIII-homologous domains (*C1* and *C2*), arginine–glycine–aspartic acid (*RGD*).

Materials and Methods

Preparation of Lactadherin-Bearing Sonazoid Bubbles

Sonazoid bubbles (1.2×10^8 bubbles/100 μl) were incubated with 0, 0.1, 1, 2, 5, or 10 μg phycoerythrin (PE)-labeled recombinant human MFG-E8/lactadherin (2767-MF, R&D systems, Inc., Minneapolis, MN) in microtubes for 15 min at room temperature. PE-labeling of lactadherin was performed using an R-phycoerythrin labeling kit (LK23, Dojindo Laboratories, Kumamoto, Japan). The concentration of lactadherin after PE-labeling was 0.1 mg/ml, and the added volume of lactadherin was set at 100 μl. After incubation with PE-lactadherin, the bubble suspension was washed with sterile water, and centrifuged (100×*g*, 1 min). The washing process was repeated. Then, Sonazoid bubbles were assessed using a FACSCalibur (BD Bioscience, San Jose, CA) with 50,000 counts. Mean fluorescence intensity was calculated from the fluorescence histogram.

Secondly, Sonazoid bubbles incubated only with 100 μl PE-dye (equivalent of 5 μg PE-lactadherin) were also assessed to examine the nonspecific binding of PE dye with Sonazoid bubbles. Finally, FACS analysis was repeated after violent shaking to examine the stability of binding between Sonazoid bubbles and PE-lactadherin. All FACS studies were performed three times.

Effect of Conjugation with Lactadherin on Size of Sonazoid Bubbles

The size distribution of Sonazoid bubbles that were incubated with 5 μg lactadherin (Sonazoid–lactadherin) was determined using the electrozone sensing method (Multisizer III, Beckman Coulter, Inc., Fullerton, CA). Prior to measurement, bubbles were diluted 1,000-fold with Coulter Isoton II diluent (Beckman Coulter). The mean and median diameters were calculated from the histogram of the volume-weighted size distribution of 50,000 bubbles. As a control, the size distribution of Sonazoid bubbles incubated with 100 μl saline (Sonazoid–phosphate-buffered saline (PBS)) was also determined.

Acoustic Property of Sonazoid–Lactadherin

To compare the acoustic property of Sonazoid–lactadherin with Sonazoid–PBS, *in vitro* experiments were performed, as previously reported [15]. Briefly, bubble suspension (1 ml; 1×10^3, 1×10^4, 1×10^5, and 1×10^6 bubbles/ml) was added to the sample wells of a custom-made 2 % (*w/v*) agarose mold, then real-time (frame rate, 30 Hz) ultrasound images were acquired with a clinical ultrasound scanner system (SONOS 5500, Philips Healthcare, Bothell, WA) equipped with a 15–6-l probe (6–15 MHz). The acoustic power was set at −20 dB, which corresponds to a mechanical index of 0.1. The image depth was set at 4 cm. The position of focus was set at the center of the agarose mold, and the overall gain setting was optimized at the beginning of the experiment and kept constant throughout the experiment. Acquired contrast images were transferred to an off-line computer (QLab, Philips Healthcare) to measure the baseline-subtracted video intensity at each experimental setting.

Cell Culture

Human umbilical vein endothelial cells (HUVEC) were purchased from Lonza (Walkersville, MD) and utilized as positive control cells that express integrin αvβ3 on their surface. HUVEC were cultured in EBM-2 medium supplemented with an EGM-2 bullet kit (Lonza). All studies were examined at passage 3 or 4. For the parallel plate flow chamber study, HUVEC were seeded on 33-mmΦ glass cover slips.

Flow Cytometry

Firstly, the expression of integrin αvβ3 on the surface of HUVEC was confirmed. Anti-human integrin αvβ3 (MAB1976Z; Millipore Co., Billerica, MA) or isotype control mouse IgG_1 (CBL600; Millipore) antibodies were labeled using a Zenon® Alexa Fluor® 488 mouse IgG_1 labeling kit (Z25002; Invitrogen). After harvesting with cell dissociation buffer (13150–016; Invitrogen) with collagenase (032–10534; Wako Pure Chemical Industries, Ltd., Osaka, Japan), 5×10^5 HUVEC were incubated with 2 μg integrin αvβ3 or isotope control antibodies for 30 min at room temperature. After washing and centrifugation twice, HUVEC were labeled with 7AAD (BD Biosciences, San Jose, CA), and 10,000 viable cells were analyzed using a FACSCalibur.

Secondly, we examined whether lactadherin is able to attach to integrin αvβ3 on HUVEC. Dispersed HUVEC were incubated with 2 μg PE-labeled lactadherin for 15 min at room temperature. After washing and centrifugation twice, HUVEC labeled with 7AAD were analyzed by FACSCalibur. To examine the nonspecific binding of PE dye with HUVEC, HUVEC incubated only with an equal amount of PE dye (equivalent of 2 μg PE-lactadherin) were also analyzed.

Specificity of Binding Between Lactadherin and HUVEC

To clarify the specificity of binding between lactadherin and HUVEC, experiments with solid-phase ELISA were performed [16]. The 96-well Maxisorp plates (439454, Thermo Fisher Scientific, Inc., Waltham, MA) were coated with lactadherin (10 μg/ml in PBS) by incubating them overnight at 4 °C with 50 μl/well. The wells were blocked with 7.5 % bovine serum albumin (BSA, A9418, Sigma-Aldrich Co., St. Louis, MO) for 4 h at 4 °C. Detached HUVEC was suspended in EBM-2 medium containing 1 % BSA, and then incubated with anti-integrin αvβ3 antibody (10 μg/ml) or cRGD peptide (10 and 100 μg/ml, Bachem AG, Bubendorf, Switzerland) for 30 min at room temperature. After washing, cells were resuspended at 4×10^5 cells/ml in EBM-2 medium containing 1 % BSA, then 100 μl cell suspension was added to each well. The plates were incubated for 15 min at room temperature. After washing with PBS to remove the unattached cells, the attached cells were fixed with 1 % glutalaldehyde for 10 min, stained with 0.1 % crystal violet for 20 min at room temperature. The cells were lysed with 50 μl of Triton X-100 (0.5 %), and the absorbance (595 nm) was measured by microplate reader (model 680, Bio-Rad Laboratories, Hercules, CA). Additionally, the adherent HUVEC was visualized microscopically after staining with crystal violet. Binding assay was carried out three times in triplicate.

Parallel Plate Flow Chamber Assay

The adhesion of Sonazoid bubbles to HUVEC was assessed using a parallel plate flow chamber system (Glycotech, Gaithersburg, MD) [17]. The silicon gasket used in this study has a width of 2.5 mm and a height of 0.254 mm (Gasket B). Cover slips of 33 mmΦ were mounted in the chamber and placed in an inverted position to maximize the interaction between HUVEC and bubbles. Bubble dilution and washing of the flow chamber were performed with fetal bovine serum-reduced EGM-2 medium (0.5 %). After 2 min of washing of the flow chamber system, 5×10^6/ml of bubbles were drawn through the chamber at a shear stress of 0.7 dynes/cm^2 over 4 min, followed by rinsing for 6 min. The number of bubbles that adhered in 15 fields of view (FOV; 273 × 362 μm) was determined under a microscope (Biorevo BZ-9000; Keyence Co., Osaka, Japan) equipped with a ×40 objective lens. Flow chamber studies were performed three times.

Statistical Analysis

All data were expressed as mean ± standard deviation. For comparison between two groups, Student's unpaired *t* test was applied. Comparison among the three groups was performed by analysis of variance followed by post hoc Tukey–Kramer test. A *p* value less than 0.05 was considered to indicate statistical significance for all comparisons.

Results

Representative FACS histograms of Sonazoid bubbles after incubation with PE-lactadherin are shown in Fig. 2a. Higher mean fluorescence intensity was observed by increasing the dose of lactadherin (0 μg [3.1±0.1] vs. 0.1 μg [10.4±1.1] vs. 1 μg [60.1±7.3] vs. 2 μg [113.8±19.2] vs. 5 μg [159.9±10.1] (Fig. 2d). However, mean fluorescence intensity was significantly decreased by increasing the lactadherin dose to 10 μg [118.9± 10.9] (Fig. 2d). PE-positive Sonazoid bubbles were detected even after incubation only with PE dye (Fig. 2b). However, the fluorescence intensity of PE dye-bearing Sonazoid bubbles was significantly lower than that of PE-lactadherin-bearing Sonazoid bubbles (51.3±4.2 vs. 159.9±10.1) (Fig. 2d). Because the binding between Sonazoid bubbles and lactadherin was robust, the histogram of FACS analysis and mean fluorescence intensity did not change even after violent shaking (before shaking; 159.9± 10.1 vs. after shaking; 152.7±8.1) (Fig. 2c, d)

Representative histograms of Sonazoid–PBS and Sonazoid–lactadherin are shown in Fig. 3a. The size distribution of Sonazoid bubbles was not altered even after conjugation with lactadherin. In quantitative analysis, the size of Sonazoid bubbles slightly decreased during the process of washing and centrifugation (untreated Sonazoid, 2.97±0.01 μm vs. Sonazoid–PBS, 2.90±0.04 μm mean diameter, untreated Sonazoid, 2.80±0.01 μm vs. Sonazoid–PBS, 2.75±0.03 μm median diameter). However, the mean and median diameters of Sonazoid bubbles were not increased even after conjugation with lactadherin (Sonazoid–lactadherin, 2.81±0.02 μm mean diameter and 2.69±0.02 μm median diameter) (Fig. 3b).

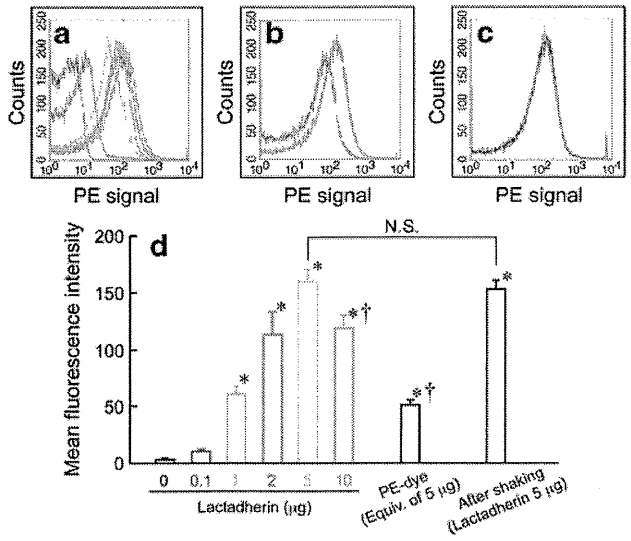

Fig. 2. Binding between Sonazoid bubbles and lactadherin. **a** PE signals derived from Sonazoid bubbles increased concomitantly with the added dose of PE-lactadherin; 0 μg, *black*; 0.1 μg, *red*; 1 μg, *green*; 2 μg, *pink*; 5 μg, *blue*; 10 μg, *orange line*. **b** Compared to incubation with PE dye, a higher PE signal was observed after incubation with PE-lactadherin. *Black line*, PE dye; *red line*, PE-lactadherin. **c** Binding between lactadherin and Sonazoid bubbles was maintained even after violent shaking. *Black line*, before shaking; *red line*, after shaking. **d** Quantitative analysis of fluorescence intensity. **P*<0.05 vs. 0 μg lactadherin, †*P*<0.05 vs. 5 μg lactadherin. *N.S.* not significant.

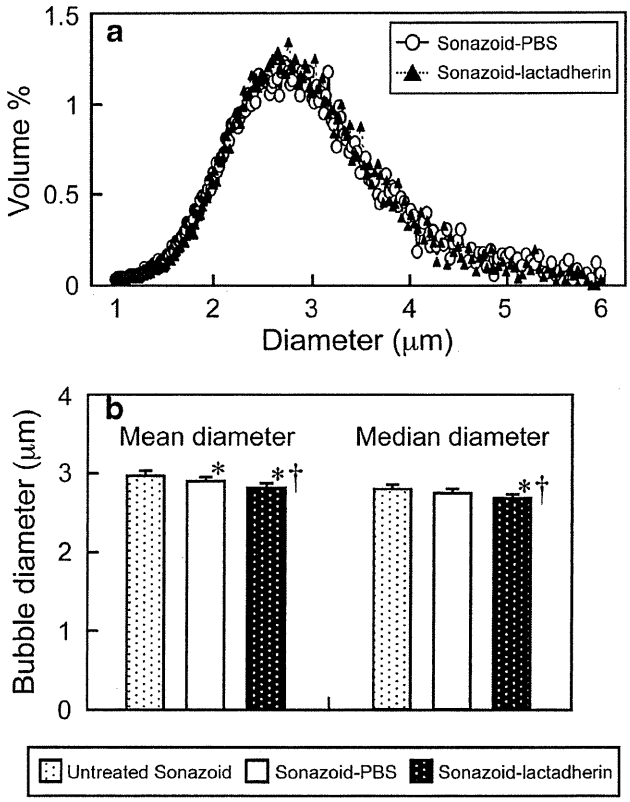

Fig. 3. Size distribution and diameters of Sonazoid bubbles. **a** The histogram of bubble size distribution was almost the same even after conjugation with lactadherin. **b** Even after conjugation with lactadherin, the mean and median diameters of Sonazoid bubbles were not increased. **P*<0.05 vs. Untreated Sonazoid, †*P*<0.05 vs. Sonazoid–PBS.

Representative ultrasound images of Sonazoid–PBS and Sonazoid–lactadherin are shown in Fig. 4a. The video intensity was increased concomitant with the dose of bubbles, irrespective of the incubation with lactadherin (Sonazoid–PBS, 6.9±5.8 vs. 21.5±3.1 vs. 69.8±2.0 vs. 115.0±2.0; Sonazoid–lactadherin, 10.2±3.9 vs. 35.5±3.6 vs. 82.3±5.8 vs. 113.4±1.4) (Fig. 4b). It was noteworthy that the acoustic property of Sonazoid bubbles was not impaired even after incubation with lactadherin.

The expression of integrin αvβ3 on HUVEC was supported by the significantly higher fluorescence intensity after incubation with anti-integrin αvβ3 antibody (Fig. 5a). Binding between HUVEC and PE-lactadherin was also examined by FACS analysis. Although a slight increase in the PE signal was observed even after conjugating HUVEC with PE dye, the mean fluorescence intensity after incubation with PE-lactadherin was significantly higher than that after incubation with PE dye (HUVEC; 3.2±0.3 vs. PE dye; 13.6±1.2 vs. lactadherin; 127.4± 12.9) (Fig. 5b). This result indicates that binding between lactadherin and integrin αvβ3-expressing HUVEC is feasible.

Representative photographs of adherent HUVEC to lactadherin are summarized in Fig. 6a. Although the adherent HUVEC were hardly detected in the absence of lactadherin, a lot of HUVEC adhered to lactadherin-coated well (optical density; 0.007±0.001 vs. 0.115±0.019) (Fig. 6b). However, the number of adherent HUVEC to lactadherin was significantly decreased by pre-incubating with anti-integrin αvβ3 antibody or cRGD peptide (0.071±0.003 in anti-integrin αvβ3, 0.054±0.025 in 100 μg/ml cRGD, respectively).

Figure 7a shows representative images of HUVEC perfused with Sonazoid–PBS or Sonazoid–lactadherin under shear flow. Compared to perfusion with Sonazoid–PBS, a large number of adherent bubbles were observed on HUVEC after perfusion with Sonazoid–lactadherin. In quantitative analysis, the number of adherent bubbles was increased about fivefold with the intermediation of lactadherin (12.1±6.0 vs. 58.7±33.1 bubbles/FOV) (Fig. 7b).

Discussion

PS is well-known as an important molecule for the clearance of apoptotic cells, and several kinds of proteins that bind with PS have been discovered [18, 19]. Among them, it has been established that lactadherin binds with PS in a Ca^{2+}-independent manner [13, 14]. As we expected, the synthesis of lactadherin-bearing Sonazoid bubbles was feasible without requiring the addition of Ca^{2+} (Fig. 2a), and the binding between PS in Sonazoid and lactadherin was robust even after violent shaking (Fig. 2c) [8]. It was noteworthy that the

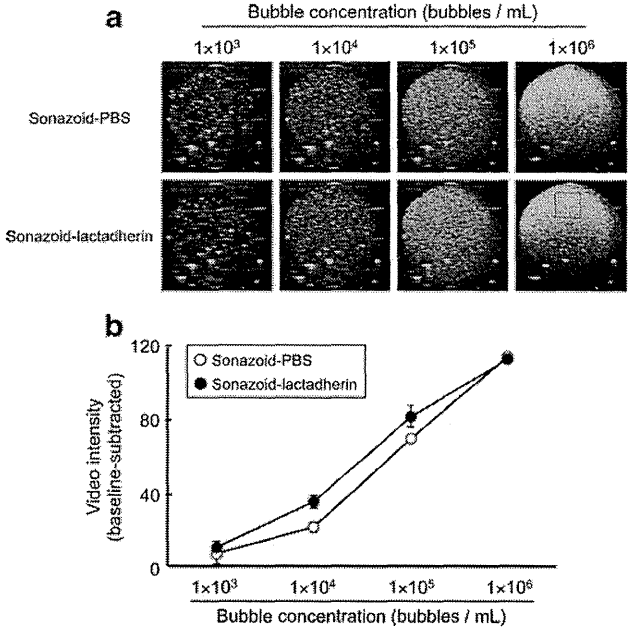

Fig. 4. Comparison of acoustic property of Sonazoid with or without lactadherin conjugation. **a** Representative ultrasound images at each bubble concentration. The region of interest is shown in a *red square*. **b** Baseline-subtracted video intensity at each experimental setting. The acoustic property of Sonazoid was not impaired even after incubation with lactadherin.

size of bubbles was not increased even after incubation with lactadherin (Fig. 3a, b). Additionally, the acoustic property of Sonazoid–lactadhrin was comparable to that of Sonazoid–PBS (Fig. 4). These results imply that an intravenous infusion of lactadherin-bearing Sonazoid bubbles would have little risk of embolization and yield sufficient contrast enhancement. As shown in Fig. 7, lactadherin augmented the number of Sonazoid bubbles adherent to integrin αvβ3-expressing endothelial cells. Furthermore, the specificity of binding between lactadherin and integrin αvβ3 on HUVEC was also confirmed (Fig. 6). Taken together, our results imply that lactadherin-bearing Sonazoid bubbles have potential as a novel and easy-to-prepare ultrasound contrast agent for detecting integrin αvβ3-expressing cells in ultrasound molecular imaging.

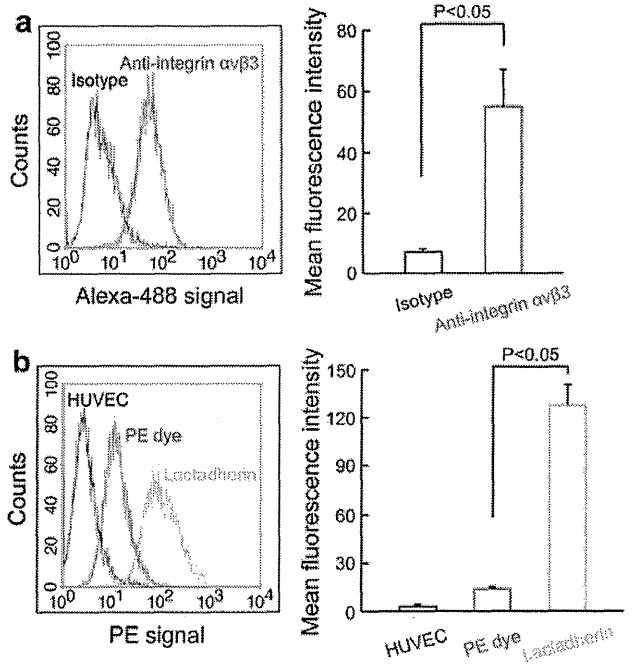

Fig. 5. Binding between integrin αvβ3-expressing HUVEC and lactadherin. **a** The fluorescence intensity derived from HUVEC after incubation with anti-integrin αvβ3 antibody was significantly higher than that after incubation with isotype control (55.0±12.2 vs. 7.1±0.7) (n=3). **b** A significant increase in mean fluorescence intensity was observed by conjugating HUVEC with PE-lactadherin (n=6).

In our previous study, we demonstrated the feasibility of antibody-carrying bubbles preparation based on Sonazoid via annexin V and biotin–avidin complex formation [7]. However, the addition of Ca^{2+}, which is necessary for binding between annexin V and PS, resulted in the obvious bubble aggregation and bubble loss. Additionally, the binding between annexin V and PS was quite fragile. Fortunately, this was not the case with lactadherin because lactadherin binds with PS in a Ca^{2+}-independent manner (Fig. 2c). In this regard, lactadherin is superior to annexin V as a mediator for detecting PS in Sonazoid.

As well as vascular endothelial growth factor (VEGF) and VEGF receptors, integrins have been identified as target molecules for imaging of angiogenesis [20, 21]. Integrin αvβ3, one of the integrin families, has been considered a useful molecule for detecting tumor angiogenesis because integrin αvβ3 is known to play a key role in angiogenesis [22]. In ultrasound molecular imaging, several studies of integrin-targeted imaging have been performed by conjugating echistatin, RGD peptides, and antibodies on the surface of bubbles [23–26]. The majority of targeted bubbles have utilized streptavidin as a

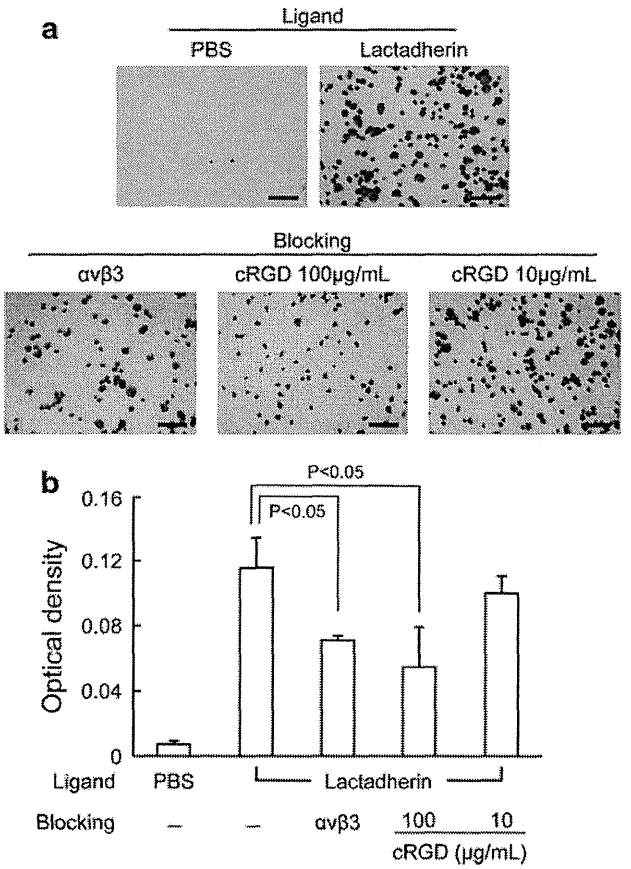

Fig. 6. Adhesion of HUVEC to the lactadherin-coated plates. **a** Representative photographs of adherent HUVEC at each experimental setting. Scale bars = 100 μm. **b** Optical density was significantly decreased by pre-incubating HUVEC with anti-integrin αvβ3 antibody or cRGD peptide.

mediator for conjugating antibodies or peptides onto the surface of bubbles. However, the clinical application of streptavidin-conjugated microbubbles would be difficult due to immunogenicity [27]. To overcome this issue, clinically translatable bubbles that do not contain streptavidin have been developed recently [28–31]. In addition to the nonuse of streptavidin for targeted bubble preparation, the utilization of a clinically available ultrasound contrast agent is the prime advantage of our approach. In this regard, lactadherin-bearing Sonazoid bubbles might lower the barrier for the clinical translation of targeted bubbles.

Weaknesses of Lactadherin-Bearing Sonazoid Bubbles

To improve the flexibility, hydrophilicity, and targetability of targeted bubbles, the majority of recently developed targeted bubbles project antibodies or peptides away from the surface of the bubble shell by means of a polyethylene glycol arm [3, 32–34]. In contrast, lactadherin binds directly with PS in the shell of Sonazoid bubbles in our approach (Fig. 1). As shown in Fig. 5, a larger number of Sonazoid bubbles were adherent to HUVEC by the intermediation of lactadherin in the flow chamber study. However, the flexibility and targetability of lactadherin-bearing Sonazoid bubbles might be lower than those of other conventional targeted bubbles. Additionally, the surface density of lactadherin (i.e., RGD motif) might also be low. Considering these issues, further study examining an alternative approach that utilizes lactadherin as a mediator to attach antibodies or peptides on the surface of Sonazoid bubbles would be beneficial.

With regard to the administration of lactadherin in an *in vivo* study, Asano et al. reported the possibility of autoantibody production by administration of an excess amount of lactadherin in mice [35]. Therefore, the optimal preparation method with minimum use of lactadherin should be established in a future study for the *in vivo* and clinical translation of lactadherin-bearing Sonazoid bubbles.

Study Limitation

In addition to the bubble size determination, the concentration of bubbles after the preparation of targeted Sonazoid bubbles was also determined using Multisizer III (n=3). As a result, the bubble concentration was decreased to one fifth due to dilution of the bubble suspension (untreated Sonazoid, $9.5\pm0.2 \times 10^8$ bubbles/ml vs. Sonazoid–PBS, $2.0\pm0.1 \times 10^8$ bubbles/ml)

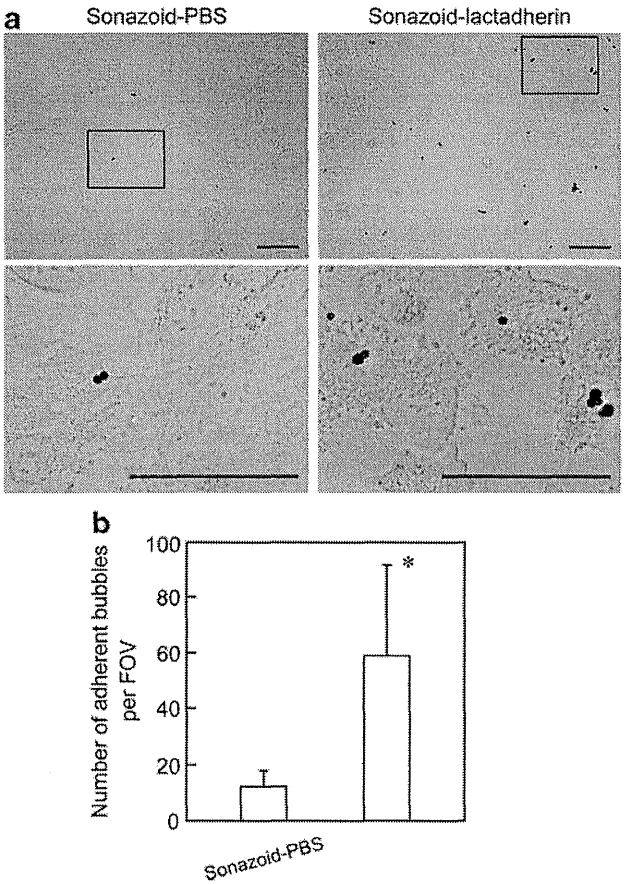

Fig. 7. Adhesion of Sonazoid bubbles to HUVEC under shear flow with or without the intermediation of lactadherin. **a** The number of Sonazoid bubbles adherent to HUVEC was increased by the intermediation of lactadherin. The *boxed areas* in *upper panels* are shown at higher magnification in *lower panels*. Scale bars = 50 μm. **b** Quantitative analysis of adherent bubbles per field of view. *FOV* field of view. *$P<0.05$ vs. Sonazoid–PBS.

(Supplementary Fig. 1a). Additionally, the decrease in bubble concentration was further enhanced by incubation with lactadherin (Sonazoid–lactadherin, $1.1\pm0.1 \times 10^8$ bubbles/ml) due to adhesion of bubbles to the wall of microtubes (Supplementary Fig. 1b). However, this loss of bubbles could partly be avoidable by coating the surface of the microtubes with 2-methacryloyloxyethyl phosphorylcholine polymer (NOF Corp., Tokyo, Japan) to suppress protein adsorption (data not shown). Furthermore, the use of glass tubes for targeted bubble preparation might further avoid the loss of bubbles. Ideally, omission of the washing process would be desirable for easy preparation of targeted bubbles. Therefore, further study regarding the development of lactadherin-bearing Sonazoid bubbles without the washing process would be beneficial.

Although the feasibility of lactadherin-bearing Sonazoid bubbles as targeted contrast agent for integrin αvβ3 was demonstrated, the potential of lactadherin-bearing Sonazoid bubbles to visualize the neovascularization *in vivo* is still unknown. Therefore, further study examining the diagnostic utility of lactadherin-bearing Sonazoid bubbles in animal models of tumor or therapeutic angiogenesis should be required.

Conclusion

In the present study, we demonstrated that adhesion of Sonazoid bubbles to integrin αvβ3-expressing endothelial cells was augmented through the intermediation of lactadherin. Lactadherin-bearing Sonazoid bubbles might be a useful contrast agent for tumors or therapeutic angiogenesis in both basic and clinical ultrasound molecular imaging in the near future.

Acknowledgments. This study was supported by a Grant-in-Aid for Young Scientists (B) from the Ministry of Education, Culture, Sports, Science and Technology (MEXT).

Conflict of interest. The authors declare that they have no conflict of interest.

References

1. Villanueva FS, Wagner WR (2008) Ultrasound molecular imaging of cardiovascular disease. Nat Clin Pract Cardiovasc Med 5:S26–32
2. Chadderdon SM, Kaul S (2010) Molecular imaging with contrast enhanced ultrasound. J Nucl Cardiol 17:667–677
3. Leong-Poi H (2009) Molecular imaging using contrast-enhanced ultrasound: evaluation of angiogenesis and cell therapy. Cardiovasc Res 84:190–200
4. Deshpande N, Pysz MA, Willmann JK (2010) Molecular ultrasound assessment of tumor angiogenesis. Angiogenesis 13:175–188

5. Sontum PC (2008) Physicochemical characteristics of Sonazoid, a new contrast agent for ultrasound imaging. Ultrasound Med Biol 34:824–833
6. Lindner JR, Song J, Xu F et al (2000) Noninvasive ultrasound imaging of inflammation using microbubbles targeted to activated leukocytes. Circulation 102:2745–2750
7. Otani K, Yamahara K (2011) Development of antibody-carrying microbubbles based on clinically available ultrasound contrast agent for targeted molecular imaging: a preliminary chemical study. Mol Imaging Biol 13:250–256
8. Otani K (2011) Feasibility of clinical application of ultrasound molecular imaging. In: Minin IV, Minin OV (eds) Ultrasound imaging—medical applications. InTech, Rijeka, Croatia, pp 295–312
9. Stubbs JD, Lekutis C, Singer KL et al (1990) cDNA cloning of a mouse mammary epithelial cell surface protein reveals the existence of epidermal growth factor-like domains linked to factor VIII-like sequences. Proc Natl Acad Sci U S A 87:8417–8421
10. Andersen MH, Graversen H, Fedosov SN et al (2000) Functional analyses of two cellular binding domains of bovine lactadherin. Biochemistry 39:6200–6206
11. Hanayama R, Tanaka M, Miwa K et al (2002) Identification of a factor that links apoptotic cells to phagocytes. Nature 417:182–187
12. Yamaguchi H, Takagi J, Miyamae T et al (2008) Milk fat globule EGF factor 8 in the serum of human patients of systemic lupus erythematosus. J Leukoc Biol 83:1300–1307
13. Shi J, Gilbert GE (2003) Lactadherin inhibits enzyme complexes of blood coagulation by competing for phospholipid-binding sites. Blood 101:2628–2636
14. Dasgupta SK, Guchhait P, Thiagarajan P (2006) Lactadherin binding and phosphatidylserine expression on cell surface-comparison with annexin A5. Transl Res 148:19–25
15. Yin T, Wang P, Zheng R et al (2012) Nanobubbles for enhanced ultrasound imaging of tumors. Int J Nanomedicine 7:895–904
16. Lechner AM, Assfalg-Machleidt I, Zahler S et al (2006) RGD-dependent binding of procathepsin X to integrin alphavbeta3 mediates cell-adhesive properties. J Biol Chem 281:39588–39597
17. Leong-Poi H, Christiansen J, Heppner P et al (2005) Assessment of endogenous and therapeutic arteriogenesis by contrast ultrasound molecular imaging of integrin expression. Circulation 111:3248–3254
18. Wu Y, Tibrewal N, Birge RB (2006) Phosphatidylserine recognition by phagocytes: a view to a kill. Trends Cell Biol 16:189–197
19. Nagata S, Hanayama R, Kawane K (2010) Autoimmunity and the clearance of dead cells. Cell 140:619–630
20. Cai W, Niu G, Chen X (2008) Imaging of integrins as biomarkers for tumor angiogenesis. Curr Pharm Des 14:2943–2973
21. Dobrucki LW, de Muinck ED, Lindner JR et al (2010) Approaches to multimodality imaging of angiogenesis. J Nucl Med 51:66S–79S
22. Friedlander M, Brooks PC, Shaffer RW et al (1995) Definition of two angiogenic pathways by distinct alpha v integrins. Science 270:1500–1502
23. Ellegala DB, Leong-Poi H, Carpenter JE et al (2003) Imaging tumor angiogenesis with contrast ultrasound and microbubbles targeted to alpha(v)beta3. Circulation 108:336–341
24. Leong-Poi H, Christiansen J, Klibanov AL et al (2003) Noninvasive assessment of angiogenesis by ultrasound and microbubbles targeted to alpha(v)-integrins. Circulation 107:455–460
25. Dayton PA, Pearson D, Clark J et al (2004) Ultrasonic analysis of peptide- and antibody-targeted microbubble contrast agents for molecular imaging of alphavbeta3-expressing cells. Mol Imaging 3:125–134
26. Palmowski M, Huppert J, Ladewig G et al (2008) Molecular profiling of angiogenesis with targeted ultrasound imaging: early assessment of antiangiogenic therapy effects. Mol Cancer Ther 7:101–109
27. Carter P (2001) Improving the efficacy of antibody-based cancer therapies. Nat Rev Cancer 1:118–129
28. Pochon S, Tardy I, Bussat P et al (2010) BR55: a lipopeptide-based VEGFR2-targeted ultrasound contrast agent for molecular imaging of angiogenesis. Invest Radiol 45:89–95
29. Pysz MA, Foygel K, Rosenberg J et al (2010) Antiangiogenic cancer therapy: monitoring with molecular US and a clinically translatable contrast agent (BR55). Radiology 256:519–527
30. Anderson CR, Rychak JJ, Backer M et al (2010) scVEGF microbubble ultrasound contrast agents: a novel probe for ultrasound molecular imaging of tumor angiogenesis. Invest Radiol 45:579–585
31. Anderson CR, Hu X, Zhang H et al (2011) Ultrasound molecular imaging of tumor angiogenesis with an integrin targeted microbubble contrast agent. Invest Radiol 46:215–224
32. Lindner JR (2009) Molecular imaging of cardiovascular disease with contrast-enhanced ultrasonography. Nat Rev Cardiol 6:475–481
33. Lindner JR (2010) Molecular imaging of vascular phenotype in cardiovascular disease: new diagnostic opportunities on the horizon. J Am Soc Echocardiogr 23:343–350
34. Klibanov AL (2006) Microbubble contrast agents: targeted ultrasound imaging and ultrasound-assisted drug-delivery applications. Invest Radiol 41:354–362
35. Asano K, Miwa M, Miwa K et al (2004) Masking of phosphatidylserine inhibits apoptotic cell engulfment and induces autoantibody production in mice. J Exp Med 200:459–467

Int J Hematol (2014) 99:463–470
DOI 10.1007/s12185-014-1542-x

ORIGINAL ARTICLE

Soluble interleukin-2 receptor level on day 7 as a predictor of graft-versus-host disease after HLA-haploidentical stem cell transplantation using reduced-intensity conditioning

Katsuji Kaida · Kazuhiro Ikegame · Junko Ikemoto · Rie Murata · Reiko Irie · Satoshi Yoshihara · Shinichi Ishii · Masaya Okada · Takayuki Inoue · Hiroya Tamaki · Toshihiro Soma · Yoshihiro Fujimori · Shunro Kai · Hiroyasu Ogawa

Received: 9 December 2013 / Revised: 13 February 2014 / Accepted: 13 February 2014 / Published online: 6 March 2014

Abstract In the present study, we analyzed the kinetics of serum soluble interleukin-2 receptor (sIL-2R) using data from 77 patients undergoing HLA-haploidentical transplantation using reduced-intensity conditioning (RIC), who were at an advanced stage or at high risk for relapse, to clarify the usefulness of sIL-2R as a biomarker of acute graft-versus-host disease (GVHD). Anti-T-lymphocyte globulin and methylprednisolone were used as GVHD prophylaxis. While the median sIL-2R in 38 patients not developing GVHD was suppressed at levels <740 U/ml, sIL-2R in 25 patients developing severe GVHD peaked on day 11 (1,663 U/ml), and thereafter decreased to <1,000 U/ml after day 30. The occurrence of GVHD was not limited to times of high sIL-2R level, but occurred at any time point on the sIL-2R curve. Most patients developing GVHD, however, experienced a higher sIL-2R level early in their transplant course. The combination of RIC and glucocorticoids sufficiently suppressed sIL-2R levels after HLA-haploidentical transplantation. In a multivariate analysis to identify factors associated with GVHD, day 7 sIL-2R >810 U/ml was the only factor significantly associated with the occurrence of severe GVHD ($p = 0.0101$).

Keywords Allogeneic stem cell transplantation · Graft-versus-host disease · Soluble interleukin-2 receptor · Alloreactive response · HLA-haploidentical transplantation

Katsuji Kaida and Kazuhiro Ikegame contributed equally.

K. Kaida · K. Ikegame · S. Yoshihara · S. Ishii · M. Okada · T. Inoue · H. Tamaki · T. Soma · H. Ogawa (✉)
Division of Hematology, Department of Internal Medicine, Hyogo College of Medicine, 1-1 Mukogawa-cho, Nishinomiya, Hyogo 663-8501, Japan
e-mail: ogawah@hyo-med.ac.jp

J. Ikemoto · R. Murata · R. Irie · Y. Fujimori · S. Kai
Department of Transfusion Medicine, Hyogo College of Medicine, Nishinomiya, Hyogo, Japan

Introduction

Bone marrow transplantation (BMT) from siblings genotypically matched for human leukocyte antigen (HLA) improves long-term survival in patients with hematologic malignancies [1]. However, more than 70 % of patients who could benefit from allogeneic BMT do not have a matched sibling donor. On the other hand, there is a >90 % chance of promptly identifying an HLA-haploidentical donor within the family; therefore, the number of patients receiving HLA-haploidentical stem cell transplantation (SCT) is gradually increasing [2–6]. The major drawback of HLA-haploidentical SCT is graft-versus-host disease (GVHD). To overcome GVHD after HLA-haploidentical SCT, several breakthroughs in transplant methodology, including drastic ex vivo T cell purging coupled with the use of megadose of stem cells [2], and in vivo T cell purging through the use of anti-T-lymphocyte globulin (ATG) [4, 5, 7], or the use of cyclophosphamide at post-transplant, have been done [6]. We and others have been studying HLA-haploidentical SCT using in vivo T cell purging method using ATG [4, 5, 7]. In this transplant setting, although the severity of GVHD is within a permissible range, GVHD still continues to be the problem, but an appropriate monitoring method of GVHD has not been established yet.

Basically, GVHD is induced by the immunological response of donor T cells. In general, once activated, T cells express the interleukin-2 receptor (IL-2R), consisting of at least three subunits (α, β and γc) on their membrane

[8, 9]. The soluble form of IL-2R is produced by proteolytic cleavage of IL-2Rα, and the release of soluble interleukin-2 receptor (sIL-2R) into the circulation has been found to be proportional to its membrane bound expression [10, 11]. Thus, serum sIL-2R levels reflect the magnitude of the T cell immunological response and are associated with the incidence and severity of GVHD in allogeneic BMT settings. In fact, sIL-2R is reported to be the most reliable biomarker among several useful biomarkers [12].

The role of sIL-2R as a GVHD biomarker has been studied mainly in the transplant settings of HLA-matched myeloablative SCT for patients mostly in complete remission (CR) [12–17]. Reduced-intensity conditioning (RIC), which has been used also in HLA-haploidentical transplant settings, may contribute to the reduction of the incidence and severity of GVHD [18–20]. We and others reported that HLA-haploidentical reduced-intensity conditioning stem cell transplantation (RIST) was useful for patients who did not have a suitable HLA-matched donor [5, 7]; however, there are no reports analyzing whether sIL-2R is still a useful biomarker of GVHD in this transplant setting.

Despite the usefulness of sIL-2R as a GVHD biomarker, transplant-related complications, including severe infection, graft rejection, and hepatic veno-occlusive disease, are known to increase sIL-2R levels [13, 15, 21]. Furthermore, leukemia- or lymphoma-associated elevation of serum sIL-2R levels has been reported [22–25]. The coexistence of these conditions could reduce the value of sIL-2R as a biomarker of GVHD.

Therefore, in the present study, after excluding data of patients with conditions that increase sIL-2R levels other than GVHD, we retrospectively studied the usefulness of sIL-2R as a GVHD biomarker using data from 77 patients, with poor prognosis or in an advanced stage of disease, who underwent HLA-haploidentical RIST.

Patients and methods

Patients

To retrospectively evaluate the role of the sIL-2R level as a biomarker of acute GVHD, we analyzed data from patients who underwent HLA-haploidentical RIST at the Hospital of Hyogo College of Medicine between January 2009 and June 2012. All patients had hematologic malignancies and were at an advanced stage or had a poor prognosis at the time of transplantation.

The inclusion criteria were as follows: donor-type engraftment, survival for at least 30 days after transplantation, the absence of hepatic veno-occlusive disease, and severe infections (CRP >10), including sepsis [13, 15, 21]. Furthermore, to avoid the effect of tumor-associated sIL-2R [22–25], data from patients who showed a tumor-associated increase in sIL-2R >2,000 U/ml before conditioning, which did not decrease to <1,000 U/ml on day 0, were excluded. Consequently, data from 20 % of the total transplant patients were excluded based on the exclusion criteria described above, and we analyzed data from 77 patients who underwent transplantation using a graft from an HLA-haploidentical donor (2–3 antigen-mismatches in GVH direction). The patients' characteristics are shown in Table 1.

Table 1 Patients' characteristics

	GVHD Grade 0	Grade I	Grade II–III
Number of patients	38	14	25
Sex			
Male/female	24/14	5/9	10/15
Age (years)			
Median (range)	42.5 (17–63)	46.5 (20–61)	55 (14–65)
Disease			
AML/MDS	17	10	12
ALL	11	0	3
Lymphoma	6	2	6
Others	4	2	4
Disease status			
Good (CR/RA/CP)	2	0	2
Intermediate (PR/RAEB/AP)	4	1	1
Poor	32	13	22
HLA disparity in GVH direction			
2 antigen	18	9	13
3 antigen	20	5	12
Number of times of transplant			
First	17	7	20
Second or later	21	7	5
Conditioning combination chemotherapy			
Busulfan-containing	8	3	9
Melphalan-containing	26	8	15
Others	4	3	1
TBI			
Containing	25	8	15
Non-containing	13	6	10

Institutional review board approval was obtained for the treatment protocol, and written informed consent was obtained from the patients and their families.

Preparative regimen for transplantation

Sixty-nine patients received a regimen consisting of fludarabine (30 mg/m^2/day on days −9 to −4), cytarabine (2 g/m^2 on days −9 to −6), ATG (thymoglobulin: total

2.5 mg/kg divided on days -3 to -1), and busulfan (4.0 mg/kg/day on days −6 and −5) or melphalan (70 mg/m^2 on days −3 and −2) with or without TBI 3–4 Gy on day 0. The remaining 8 patients received other agents instead of busulfan or melphalan because of chemoresistance. GVHD prophylaxis consisted of tacrolimus and methylprednisolone (mPSL) 1 mg/kg [5]. All patients except 2 received peripheral blood stem cells. T cell depletion was not performed.

Diagnosis of graft-versus-host disease and supportive care

Acute GVHD was graded according to standard criteria [26]. GVHD was treated as previously described [5]. Each patient was isolated in a laminar air-flow room or protective environment room, and standard decontamination procedures were followed. Oral antibiotics (ciprofloxacin, vancomycin, itraconazole or voriconazole) were administered to sterilize the bowel. Patients who were negative for cytomegalovirus (CMV) IgG received blood products from CMV-seronegative donors. Intravenous immunoglobulin was administered at a minimum dose of 100 mg/kg every 2 weeks until day 100. Cotrimoxazole was given for at least 1 year for prophylaxis of *Pneumocystis carinii* infections. Acyclovir was administered at a dose of 1,000 mg/day for 5 weeks after transplantation to prevent herpes simplex virus or varicella-zoster virus infection, and then the agent was continued for at least 2 years at a dose of 200 mg/day. Ganciclovir 7.5 mg/kg divided into 3 doses per day was administered from day −10 to day −3 as prophylaxis for CMV infection.

Measurement of serum sIL-2R

The serum sIL-2R level was monitored from the start of conditioning three times a week until hospital discharge. The serum sIL-2R concentration was evaluated using a commercially available sandwich enzyme-linked immunosorbent assay (ELISA) with two murine anti-human sIL-2R antibodies (CELLFREE Human sIL-2R ELISA Kit; Thermo Fisher Scientific Inc., Rockford, IL, USA). The normal sIL-2R level is <534 U/ml.

Statistics

The background levels of serum sIL-2R were decided using data from 38 patients who did not develop GVHD. The difference in sIL-2R levels on day 7 between patients who developed grade 0–I and grade II–III GVHD was analyzed using the Mann–Whitney *U* test. In addition, we determined the appropriate cutoff value of the sIL-2R level on day 7 to discriminate patients with and without severe GVHD through receiver operating characteristic (ROC) analysis, in which sensitivity and specificity were calculated as a function of the cutoff value, (1-specificity) was plotted against the sensitivity, and the area under the ROC curve (AUC) was calculated. Cumulative incidence of GVHD for patients with sIL-2R on day 7 of >810 or <810 U/ml was estimated using the Kaplan–Meier method, treating death and relapse as competing risks. Gray's test was used for comparison of cumulative incidence in the 2 groups. To identify factors associated with GVHD, using variables including the donor source, age, disease status before transplantation, sex, number of times of transplantation, HLA disparity in GVH direction, disease, and day 7 sIL-2R level, univariate and multivariate analyses were performed using the Cox proportional hazards model. Results were considered significant when $p \leq 0.05$. Statistical analyses were performed with EZR [27, 28].

Results

Background level of sIL-2R based on the data from patients who did not develop GVHD

Serum sIL-2R levels were monitored 3 times a week to analyze the relationship between sIL-2R levels and the development of GVHD in detail. We first identified the serum background level of sIL-2R based on data from 38 patients who did not develop acute GVHD. As shown in Fig. 1, sIL-2R was slightly high, but mostly <1,200 U/ml during 2 weeks after transplantation, and thereafter slightly decreased to <1,000 U/ml. The median value of sIL-2R

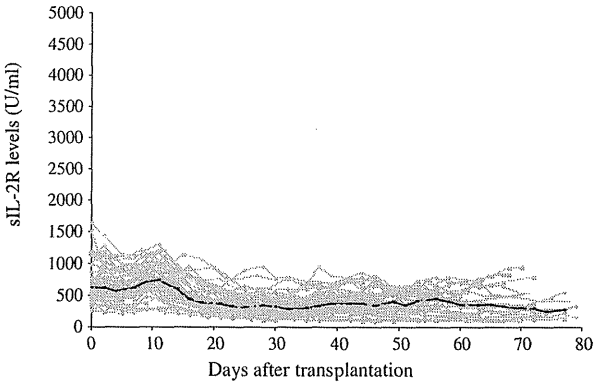

Fig. 1 The kinetics of sIL-2R in patients not developing acute GVHD. To identify the background levels of sIL-2R, changes of serum sIL-2R of 38 patients who did not develop GVHD were plotted. The normal sIL-2R level is <534 U/ml. sIL-2R was slightly high, but mostly <1,200 U/ml during 2 weeks after transplantation, and thereafter slightly decreased to <1,000 U/ml. The *bold line* shows a median sIL-2R level

was slightly increased after transplantation, peaked on day 11 (the peak level was 740 U/ml), and thereafter decreased to levels as low as between 290 and 450 U/ml.

The kinetics of sIL-2R in patients who developed severe GVHD

Next, we analyzed the kinetics of sIL-2R in 25 patients who developed severe (grade II–III) GVHD. Four patients developed skin-only GVHD, 16 gut-only GVHD, and 5 skin/gut GVHD. Those patients developed grade II–III GVHD at a median 28 days (range 3–67 days). The sIL-2R curves were found to vary patient-to-patient in the peak level or in the timing of the peak. The median sIL-2R levels increased after transplantation, reach on day 11 (the peak value of 1,663 U/ml), and thereafter decreased to low levels of <1,000 U/ml after day 30 (Fig. 2).

Regarding the relationship between the kinetics of sIL-2R and the onset of GVHD, 4 patterns were observed. Eight (32 %) patients, in whom sIL-2R increased rapidly after transplantation, developed GVHD at an increasing phase or at the peak level of sIL-2R curve by day 30 (Fig. 3a). These patients developed GVHD at a median of 9 days (range 5–26 days), with the median value of sIL-2R of 1,795 U/ml (range 1,134–4,341 U/ml) at the onset of GVHD. Four (16 %) patients developed GVHD at a decreasing phase of sIL-2R over the peak of sIL-2R (Fig. 3b). These patients developed GVHD at a median of 18.5 days (range 14–21 days), with the median value of sIL-2R of 1,465.5 U/ml (range 618–2,004 U/ml) at the onset of GVHD. Ten (40 %) patients, in whom sIL-2R increased to a high level after transplantation, with the median peak level of 1,711 U/ml (range 1,200–2,977 U/ml) at a median 5.5 days (range 0–16 days), developed GVHD after sIL-2R levels decreased to almost the normal range of sIL-2R (Fig. 3c). These patients developed GVHD at a median of 38 days (range 28–67 days), with the median value of sIL-2R of 642.5 U/ml (range 336–950 U/ml) at the onset of GVHD. Three (12 %) patients, in whom sIL-2R did not increase over the background levels of sIL-2R after transplantation, developed GVHD after day 30, when sIL-2R was slightly increasing over the background level of sIL-2R (Fig. 3d). GVHD in this group of patients occurred latest at a median of 44 days (range 37–59 days), with the median value of sIL-2R of 984 U/ml (range 935–1,054 U/ml) at the onset of GVHD. These results show that GVHD can occur on any point of the sIL-2R curve of patients with GVHD.

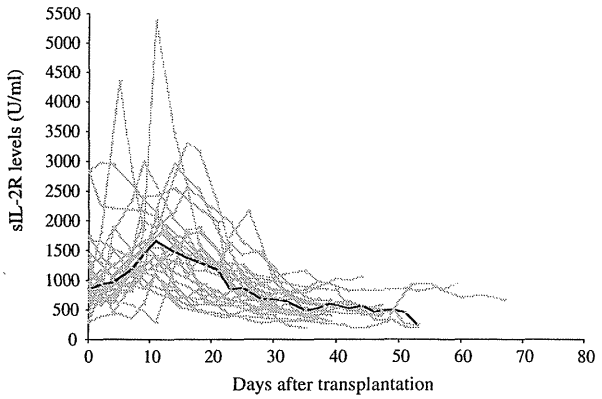

Fig. 2 The kinetics of sIL-2R in 25 patients who developed acute GVHD (grade II–III). Changes of serum sIL-2R in 25 patients who developed severe GVHD were plotted. The sIL-2R curves were found to vary patient-to-patient in the peak level or in the timing of the peak. The *bold line* shows a median sIL-2R level

Prediction of severe acute GVHD by serum sIL-2R levels on day 7

The relationship between sIL-2R change and the onset of GVHD (Fig. 3a–d) shows that the occurrence of GVHD is not limited at the time of high level of sIL-2R or at an increasing phase of sIL-2R; however, the majority of patients who developed severe GVHD showed a high level of sIL-2R early in their transplant course. Therefore, we considered that sIL-2R in the early phase of transplantation may be associated with the development of severe GVHD.

We compared sIL-2R levels on day 7 in patients who developed grade II–III GVHD or grade 0–I GVHD. Consequently, patients with grade II–III GVHD showed significantly higher sIL-2R on day 7 than those with grade 0–I GVHD ($p < 0.0001$). To determine the appropriate cutoff value of sIL-2R on day 7 to discriminate patients with and without severe GVHD, ROC analysis (Fig. 4a) was performed, and the optimal grade II–III GVHD cutoff point was found to be 810 U/ml. The area under the ROC curve (AUC) was 0.790 (CI 0.675–0.904). The relationship between the incidence of severe GVHD and day 7 sIL-2R levels was analyzed using competing risk analysis, treating death and relapse as competing risks. As shown in Fig. 4b, the cumulative incidence of severe GVHD was 43.2 % (CI 28.2–57.3 %) and 6.5 % (CI 1.1–18.9 %) for patients with day 7 sIL-2R >810 U/ml and those with day 7 sIL-2R <810 U/ml, respectively. Patients with day 7 sIL-2R >810 U/ml had a significantly higher risk of GVHD than those with day 7 sIL-2R <810 U/ml ($p = 0.00076$, log-rank test).

Next, using variables including the donor source (offspring vs others), HLA disparity (2 antigen vs 3 antigen) in the GVH direction, older age (>47 years), disease status before transplantation (CR vs non-CR), sex, number of times of transplantation, disease (ALL vs others), and day 7 sIL-2R, factors that were significantly associated with the development of severe GVHD were analyzed using the

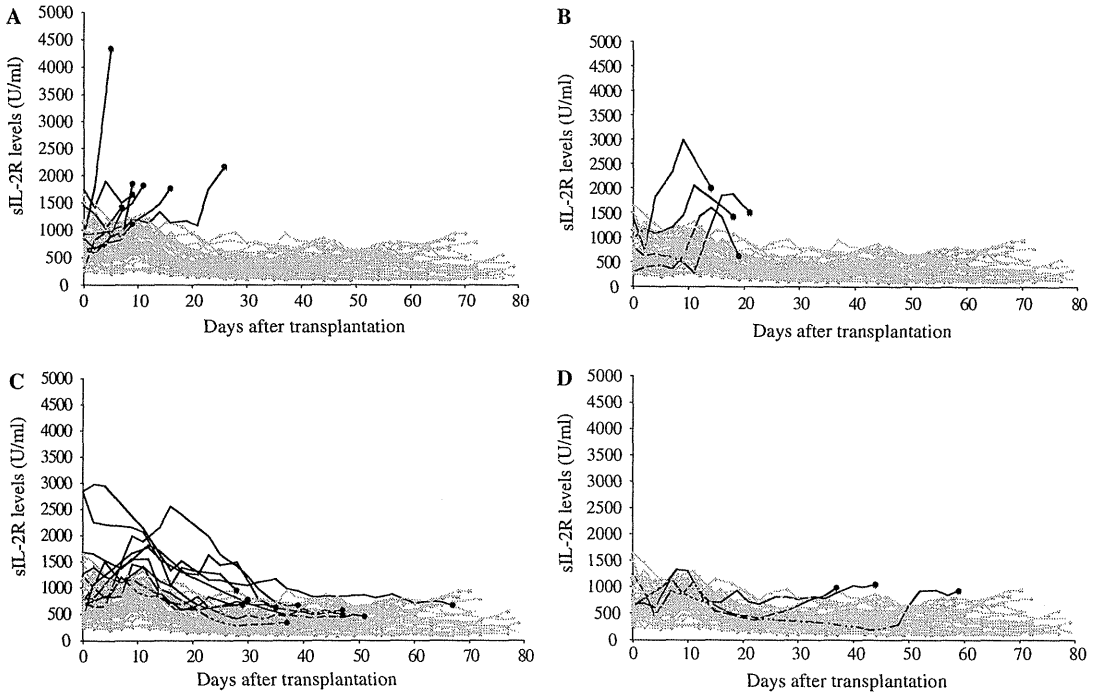

Fig. 3 The relationship between the kinetics of sIL-2R and onset of GVHD in patients who developed severe acute GVHD. *Bold lines* show changes of sIL-2R in patients who developed severe GVHD. *Closed circles*, which are at the end of the *bold lines*, show the onset of GVHD. *Gray lines* show changes of sIL-2R in patients not developing GVHD. **a** GVHD occurred at an increasing phase of sIL-2R or at the peak level by day 30. **b** GVHD occurred at a decreasing phase of sIL-2R (still at a high level) over the peak of sIL-2R. **c** GVHD occurred after returning to the background level of sIL-2R, which passed through the high levels after transplantation. **d** GVHD occurred at a time point slightly increased from the background level of sIL-2R after day 30

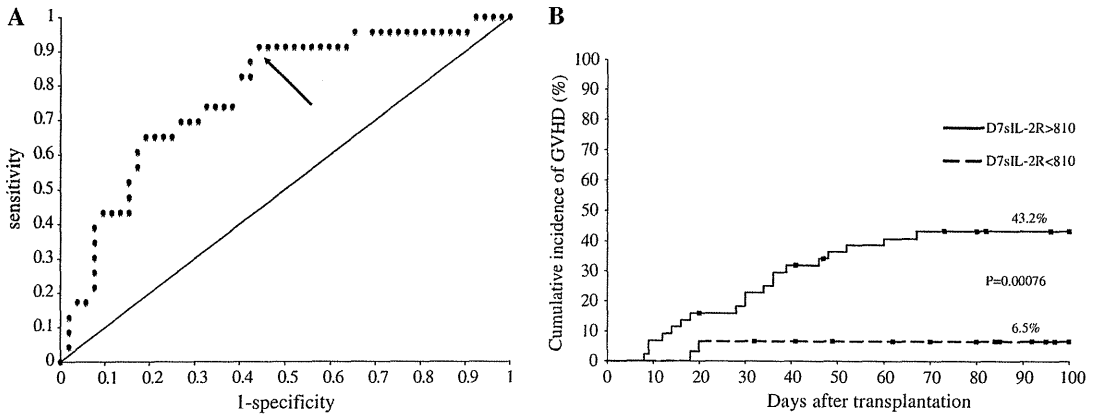

Fig. 4 **a** ROC curve of sIL-2R level on day 7 for the prediction of severe GVHD. To determine the appropriate cutoff value of sIL-2R levels on day 7 to discriminate patients with and without severe GVHD, ROC analysis was performed, and the optimal grade II–III GVHD cutoff point was found to be 810 U/ml, shown by the *arrowhead*. The area under the ROC curve (AUC) was 0.790. **b** Cumulative incidence of severe GVHD for patients with sIL-2R on day 7 of >810 and <810 U/ml. Cumulative incidence of acute GVHD for patients with sIL-2R on day 7 of >810 U/ml and <810 U/ml was estimated using the Kaplan–Meier method, treating death and relapse as competing risks. Gray's test was used for comparison of cumulative incidence in the 2 groups. Patients with sIL-2R on day 7 of >810 U/ml had a significantly higher risk of severe acute GVHD than those with day 7 sIL-2R of <810 U/ml ($p = 0.00076$, log-rank test)

Cox proportional hazards model (Table 2). In a univariate analysis, day 7 sIL-2R >810 U/ml, offspring, age >47 years, and first transplantation were significantly associated with the occurrence of severe GVHD. In a multivariate analysis, day 7 sIL-2R >810 U/ml was only a factor significantly associated with the occurrence of

Table 2 Analysis of factors related to the development of severe GVHD

	Univariate analysis		Multivariate analysis	
	p	CI	*p*	CI
sIL-2R on day 7 (>802 vs <802)	0.0024	2.214–40.431	0.0101	1.597–31.999
Donor source (offspring vs others)	0.0125	1.287–8.102	0.6601	0.238–9.617
Age (>47 vs <47 years)	0.0089	1.389–9.905	0.8337	0.144–11.068
Disease status before transplantation (CR vs non-CR)	0.7203	0.307–5.527	0.1965	0.576–14.591
Sex (female vs male)	0.1877	0.769–3.820	0.526	0.525–3.523
Number of times of transplant (retransplantation vs first transplantation)	0.0155	0.112–0.795	0.2003	0.100–1.621
HLA disparity in GVH direction (2 antigen vs 3 antigen)	0.8831	0.430–2.067	0.5993	0.322–1.922
Disease (ALL vs others)	0.2713	0.152–1.698	0.490	0.181–2.265

CI confidence interval, *CR* complete remission, *non-CR* non-complete remission

severe GVHD ($p = 0.0101$, CI 1.597–31.999). Offspring, age >47 years, and first transplantation had no significant impact on the occurrence of severe GVHD.

Discussion

In the present study, using data from 77 patients who underwent HLA-haploidentical RIST, we investigated the thorough kinetics of serum sIL-2R after transplantation to elucidate the usefulness of sIL-2R as a GVHD biomarker, and found that sIL-2R on day 7 was useful as a predictor of severe GVHD.

In the present study, data from other pathological situations that increase serum sIL-2R were excluded from the analysis. Serum sIL-2R levels reflect the magnitude of the activation and proliferation of T cells, but are not specific to the GVH reaction. This is an inevitable drawback in the diagnosis of GVHD using sIL-2R, as a non-specific T cell reaction of donor or recipient origin produces sIL-2R in some particular transplant complications, such as infection. To avoid the effect of these complications on sIL-2R analysis, other researchers also excluded data from patients with these complications, who represent 15 % of allogeneic recipients [12]. In the present study, a tumor-associated increase in sIL-2R was observed in a slightly high incidence because the majority of patients treated in our institute were in non-CR at the time of transplantation; therefore, data from a slightly higher proportion (20 %) of patients were excluded.

In the absence of GVHD, the median serum sIL-2R was slightly increased after transplantation, peaked on day 11 (the peak level was 740 U/ml), and thereafter decreased to as low as between 290 and 450 U/ml (Fig. 1). On the other hand, in the presence of GVHD, the median serum sIL-2R increased after transplantation, peaked in a median of 11 days (the peak level was 1,663 U/ml), and thereafter decreased to low levels of <600 U/ml (Fig. 2). Compared with the previous studies [14, 16], in which sIL-2R levels peaked 2–3 weeks after transplantation with the peak level of 3,000–5,000 U/ml, sIL-2R in the present study reached the peak level slightly earlier, but the peak levels were lower. The use of ATG-containing RIC regimen and the incorporation of glucocorticoids into the GVHD prophylaxis are considered to contribute to the decrease in the peak level of sIL-2R, which is probably the main reason for a low incidence of severe GVHD observed in our regimen for HLA-haploidentical RIST [5]. Miyamoto et al. [14], in the study of allogeneic SCT using myeloablative conditioning, reported that sIL-2R in patients with GVHD started to increase on day 3, and that the elevation of sIL-2R on day 3 predicted the occurrence of acute GVHD. In the present study, sIL-2R in patients with GVHD started to increase on day 7, as shown in Fig. 2. This discrepancy may be explained by the use of RIC in this study, which induces mixed chimerism status between donor and recipient in the early transplant period, retarding the start of GVH reaction.

The previous studies of sIL-2R only showed that sIL-2R peaked on weeks 2 and 3, or that the peak level of sIL-2R was associated with the severity of GVHD [14, 16]. From the analysis of the onset of GVHD, GVHD was found to occur in 4 different phases of sIL-2R curve: GVHD occurred (1) at an increasing phase or at the peak level of sIL-2R after transplantation (Fig. 3a), (2) at a decreasing phase of sIL-2R (still at a high level) over the peak of sIL-2R (Fig. 3b), (3) after returning to the background level of sIL-2R, which passed through the high levels after transplantation (Fig. 3c), and (4) at a time point slightly increased from the background level of sIL-2R after day 30 (Fig. 3d). Although the prophylactic use of glucocorticoids is considered to contribute to the reduction in sIL-2R levels, as described above, there was no difference among 4 patterns of patients with GVHD in the administration schedule of steroids until the onset of GVHD. The occurrence of GVHD in 4 different phases of sIL-2R curve of

GVHD is not limited to HLA-haploidentical RIST, but observed also in other types of allogeneic SCT, including related HLA- matched, unrelated bone marrow, and umbilical cord blood SCT (data not shown). These results show that GVHD occurs at any time point on the sIL-2R curve, indicating that sIL-2R is not a suitable marker for real-time monitoring of the development of GVHD. Host organ-associated factors [29–31], other than donor T cell activation, must be also associated with the ultimate development of GVHD.

In fact, while sIL-2R peaked at a median of 11 days in patients developing GVHD, GVHD occurred at a median of 28 days. This time lag between the peak level of sIL-2R and the onset of GVHD may be explained as follows. According to the pathophysiology of GVHD that Ferrara et al. [32] proposed, donor T cell activation precedes a series of the subsequent various immunological reactions leading to the development of GVHD. In addition, GVHD may become clinically evident as the dose of immunosuppressive agents is tapered.

On the other hand, the fact that the majority of patients developing GVHD showed a high level of sIL-2R early in their transplant course indicates that sIL-2R levels in the early transplant phase could be a predictor of severe GVHD. In a univariate analysis, day 7 sIL-2R >810 U/ml, offspring, age >47 years, and first transplantation were significantly associated with the occurrence of severe GVHD; however, in a multivariate analysis, day 7 sIL-2R >810 U/ml was only a factor significantly associated with the occurrence of severe GVHD (Table 2). Thus, for the first time, we showed that sIL-2R in the early transplant phase was useful as a GVHD predictor.

The occurrence of events, such as VOD or sepses, until day 7 may result in non-specific increase in sIL-2R on day 7, which make it unable to predict GVHD using day 7 sIL-2R; however, the predictability of GVHD by sIL-2R on day 7 is not basically affected by such pathological events that occur after day 7. Regarding non-specific increase in sIL-2R on day 7, whether we can detect or diagnose such events (inducing increase in sIL-2R) on day 7 is practically important because the GVHD predictor should not be applied if a given patient has such events and shows sIL-2R >810 U/ml. The diagnosis of VOD or severe infections is relatively easy, whereas accurate quantification of residual tumor burden that may lead to tumor-associated increase in sIL-2R may be sometimes difficult. In general, in case of tumor-associated increase, sIL-2R levels are usually high since before transplantation or during conditioning, and tend to gradually or rapidly decrease after transplantation in this early transplant period, whereas, in GVHD-associated increase, sIL-2R levels are increasing at day 7 in most cases, as shown in Fig. 2. Therefore, when applied to patients undergoing allogeneic SCT in CR status, sIL-2R will be more useful as a GVHD predictor. In addition, even if such a non-specific increase blunts the usefulness of sIL-2R as GVHD predictor, when sIL-2R levels are <810 U/ml on day 7, the incidence of GVHD is only 6.5 %, as shown in Fig. 4b, indicating that patients with such low sIL-2R levels have an extremely low risk of developing severe GVHD even in HLA-haploidentical SCT.

In conclusion, in this HLA-haploidentical SCT using the combination of ATG-containing RIC regimen and the incorporation of glucocorticoid into GVHD prophylaxis, sIL-2R levels were mostly suppressed after transplantation compared with other studies on sIL-2R, which possibly lead to a low incidence of severe GVHD. sIL-2R on day 7 was useful as a predictor of GVHD in this transplant setting.

Acknowledgments We thank the medical, nursing, and laboratory staff of the participating departments for their contributions.

Conflict of interest The authors declare no conflict of interest.

References

1. Armitage JO. Medical progress. Bone marrow transplantation. N Engl J Med. 1994;330:827–38.
2. Aversa F, Terenzi A, Tabilio A, Falzetti F, Carotti A, Ballanti S, et al. Full haplotype-mismatched hematopoietic stem-cell transplantation: a phase II study in patients with acute leukemia at high risk of relapse. J Clin Oncol. 2005;23:3447–54.
3. Di Ianni M, Falzetti F, Carotti A, Terenzi A, Castellino F, Bonifacio E, et al. Tregs prevent GVHD and promote immune reconstitution in HLA-haploidentical transplantation. Blood. 2011;117:3921–8.
4. Lu DP, Dong L, Wu T, Huang XJ, Zhang MJ, Han W, et al. Conditioning including antithymocyte globulin followed by unmanipulated HLA-mismatched/haploidentical blood and marrow transplantation can achieve comparable outcomes with HLA-identical sibling transplantation. Blood. 2006;107:3065–73.
5. Ogawa H, Ikegame K, Kaida K, Yoshihara S, Fujioka T, Taniguchi Y, et al. Unmanipulated HLA 2-3 antigen-mismatched (haploidentical) bone marrow transplantation using only pharmacological GVHD prophylaxis. Exp Hematol. 2008;36:1–8.
6. Brunstein CG, Fuchs EJ, Carter SL, Karanes C, Costa LJ, Wu J, et al. Alternative donor transplantation after reduced intensity conditioning: results of parallel phase 2 trials using partially HLA-mismatched related bone marrow or unrelated double umbilical cord blood grafts. Blood. 2011;118:282–8.
7. Lee KH, Lee JH, Lee JH, Kim DY, Seol M, Lee YS, et al. Reduced-intensity conditioning therapy with busulfan, fludarabine, and antithymocyte globulin for HLA-haploidentical hematopoietic cell transplantation in acute leukemia and myelodysplastic syndrome. Blood. 2011;118:2609–17.
8. Diamantstein T, Osawa H. The interleukin-2 receptor, its physiology and a new approach to a selective immunosuppressive therapy by anti-interleukin-2 receptor monoclonal antigen. Immunol Rev. 1986;92:5–27.
9. Minami Y, Kono T, Miyazaki T, Taniguchi T. The IL-2 receptor complex: its structure, function and target genes. Annu Rev Immunol. 1993;11:245–68.

10. Junghans RP, Waldmann TA. Metabolism of Tac (IL2Ralpha): physiology of cell surface shedding and renal catabolism, and suppression of catabolism by antibody binding. J Exp Med. 1996;183:1587–602.
11. Robb RJ, Kutny RM. Structure-function relationships for the IL 2-receptor system. IV. Analysis of the sequence and ligand-binding properties of soluble Tac protein. J Immunol. 1987;139: 855–62.
12. Paczesny S, Krijanovski OI, Braun TM, Choi SW, Clouthier SG, Kuick R, et al. A biomarker panel for acute graft-versus-host disease. Blood. 2009;113:273–8.
13. Siegert W, Josimovic-Alasevic O, Schwerdtfeger R, Baurmann H, Schmidt CA, Musch R, et al. Soluble interleukin-2 receptors in patients after bone marrow transplantation. Bone Marrow Transpl. 1990;6:97–101.
14. Miyamoto T, Akashi K, Hayashi S, Gondo H, Murakawa M, Tanimoto K, et al. Serum concentration of the soluble interleukin-2 receptor for monitoring acute graft-versus-host disease. Bone Marrow Transpl. 1996;17:185–90.
15. Foley R, Couban S, Walker I, Greene K, Chen CS, Messner H, et al. Monitoring soluble interleukin-2 receptor levels in related and unrelated donor allogeneic bone marrow transplantation. Bone Marrow Transpl. 1998;21:769–73.
16. Grimm J, Zeller W, Zander AR. Soluble interleukin-2 receptor serum levels after allogeneic bone marrow transplantation as a marker for GVHD. Bone Marrow Transpl. 1998;21:29–32.
17. Kami M, Matsumura T, Tanaka Y, Mikami Y, Miyakoshi S, Ueyama J, et al. Serum levels of soluble interleukin-2 receptor after bone marrow transplantation: a true marker of acute graft-versus-host disease. Leuk Lymphoma. 2000;38:533–40.
18. Ogawa H, Ikegame K, Soma T, Kawakami M, Tsuboi A, Kim EH, et al. Powerful graft-versus-leukemia effects exerted by HLA-haploidentical grafts engrafted with a reduced-intensity regimen for relapse following myeloablative HLA-matched transplantation. Transplantation. 2004;78:488–9.
19. Ikegame K, Kawakami M, Yamagami T, Maeda H, Onishi K, Taniguchi Y, et al. HLA-haploidentical nonmyeloablative stem cell transplantation: induction to tolerance without passing through mixed chimerism. Clin Lab Haematol. 2005;27:1–3.
20. Lee KH, Lee JH, Lee JH, Kim DY, Kim SH, Shin HJ, et al. Hematopoietic cell transplantation from an HLA-mismatched familial donor is feasible without ex vivo-T cell depletion after reduced-intensity conditioning with busulfan, fludarabine, and antithymocyte globulin. Biol Blood Marrow Transpl. 2009;15: 61–72.
21. Perkins JD, Nelson DL, Rakela J, Grambsch PM, Krom RA, et al. Soluble interleukin-2 receptor level as an indicator of liver allograft rejection. Transplantation. 1989;47:77–81.
22. Kamihira S, Atogami S, Sohda H, Momita S, Yamada Y, Tomonaga M. Significance of soluble interleukin-2 receptor levels for evaluation of the progression of adult T-cell leukemia. Cancer. 1994;73:2753–8.
23. Kalmanti M, Karamolengou K, Dimitriou H, Tosca A, Vlachonikolis I, Peraki M, et al. Serum levels of tumor necrosis factor and soluble interleukin 2 receptor as markers of disease activity and prognosis in childhood leukemia and lymphoma. Int J Hematol. 1993;57:147–52.
24. Pui CH, Ip SH, Iflah S, Behm FG, Grose BH, Dodge RK, et al. Serum interleukin 2 receptor levels in childhood acute lymphoblastic leukemia. Blood. 1988;71:1135–7.
25. Cimino G, Amadori S, Cava MC, De Sanctis V, Petti MC, Di Gregorio AO, et al. Serum interleukin-2 (IL-2), soluble IL-2 receptors and tumor necrosis factor-alfa levels are significantly increased in acute myeloid leukemia patients. Leukemia. 1991;5:32–5.
26. Glucksberg H, Storb R, Fefer A, Buckner CD, Neiman PE, Clift RA, et al. Clinical manifestations of graft-versus-host diseases in human recipients of marrow from HLA matched sibling donors. Transplantation. 1974;18:295–304.
27. Kanda Y. Investigation of the freely available easy-to-use software 'EZR' for medical statistics. Bone Marrow Transpl. 2013;48:452–8.
28. Kanda J, Atsuta Y, Wake A, Ichinohe T, Takanashi M, Morishima Y, et al. Impact of the direction of HLA mismatch on transplantation outcomes in single unrelated cord blood transplantation. Biol Blood Marrow Transpl. 2013;19:247–54.
29. Ferrara JL, Harris AC, Greenson JK, Braun TM, Holler E, Teshima T, et al. Regenerating islet-derived 3-alpha is a biomarker of gastrointestinal graft-versus-host disease. Blood. 2011;118:6702–8.
30. Paczesny S, Braun TM, Levine JE, Hogan J, Crawford J, Coffing B, et al. Elafin is a biomarker of graft-versus-host disease of the skin. Sci Transl Med. 2010;2:13ra2.
31. Paczesny S, Raiker N, Brooks S, Mumaw C. Graft-versus-host disease biomarkers: omics and personalized medicine. Int J Hematol. 2013;98:275–92.
32. Ferrara JL, Levy R, Chao NJ. Pathophysiology mechanism of acute graft-vs.-host disease [review]. Biol Blood Marrow Transpl. 1999;5:347–56.

Int J Hematol (2013) 97:287–290
DOI 10.1007/s12185-012-1231-6

CASE REPORT

Detection of donor-derived CMV-specific T cells in cerebrospinal fluid in a case of CMV meningoencephalitis after cord blood stem cell transplantation

Kazuhiro Ikegame · Ruri Kato · Tatsuya Fujioka · Masaya Okada · Katsuji Kaida · Shinichi Ishii · Satoshi Yoshihara · Takayuki Inoue · Kyoko Taniguchi · Hiroya Tamaki · Toshihiro Soma · Hiroyasu Ogawa

Received: 5 April 2012 / Revised: 26 November 2012 / Accepted: 26 November 2012 / Published online: 29 December 2012

Abstract Cytomegalovirus (CMV) meningoencephalitis is a rather rare complication after allogeneic stem cell transplantation. We describe here the case of a 59-year-old man with acute myeloid leukemia who developed CMV meningoencephalitis after cord blood transplantation. The patient presented with a sudden onset of neurological symptoms, such as convulsion, on day 37. The analysis of cerebrospinal fluid (CSF) sample revealed an increase in the number of cells, which were of donor (cord blood) origin, consisting mainly of T cells. No bacteria were detected in the CSF sample. Real-time PCR analysis revealed that the CSF sample was positive for CMV, but was negative for HHV-6, adenovirus, or BK virus. The patient was diagnosed with CMV meningoencephalitis and received cidofovir. His neurological symptoms were gradually improved and completely disappeared by day 60. CMV-specific dextramer-positive $CD8^+$ T cells were detected in the peripheral blood and CSF samples, with the frequency being much higher in the CSF. To our knowledge, this is the first report on the appearance of CMV-specific T cells in CSF samples from a patient with CMV meningoencephalitis. Cord blood-derived CMV-specific T cells may develop early after transplantation, enter the intrathecal compartment, and likely contribute to the regulation of CMV-meningoencephalitis.

K. Ikegame · R. Kato · T. Fujioka · M. Okada · K. Kaida · S. Ishii · S. Yoshihara · T. Inoue · K. Taniguchi · H. Tamaki · T. Soma · H. Ogawa (✉)
Division of Hematology, Department of Internal Medicine, Hyogo Medical College, 1-1 Mukogawa-cho, Nishinomiya, Hyogo 663-8501, Japan
e-mail: ogawah@hyo-med.ac.jp

Keywords Cytomegalovirus · Viral encephalitis · Cord blood transplantation · Dextramer

Introduction

Cytomegarovirus (CMV) meningoencephalitis (CMV-ME) is a rather rare complication, occurring in 6 % of patients with viral encephalitis after allogeneic stem cell transplantation (SCT) [1]. Recently, we had a patient with acute myeloid leukemia (AML) who developed CMV-ME after cord blood stem cell transplantation (CBT), and could, for the first time, confirm the presence of donor-derived CMV-specific CD8 T cells in the cerebrospinal fluid (CSF), using the dextramer staining procedure.

Case report

A 59-year-old Japanese man with AML (M6) evolving from myelodysplastic syndrome received a chemotherapy consisting of aclarubicin and cytarabine, and achieved complete remission morphologically, which was, however, considered as returning to refractory anemia because of the existence of deletion chromosome 20 in 17 of 20 cells in the karyotype analysis of bone marrow (BM) samples. The patient therefore was referred to our hospital for allogeneic SCT. Since there was no suitable donor in related and unrelated donor pools, we decided to perform CBT using reduced-intensity conditioning regimen, which consisted of fludarabine (FLU) 30 mg/m^2/day (day −6 to −2, total 150 mg), cyclophosphamide (CY) 50 mg/kg/day on day −6, and total body irradiation (TBI) 3 Gy on day −7 [2]. Graft-versus-host disease (GVHD) prophylaxis consisted of continuous infusion of cyclosporine (CsA) (target blood

concentration was 300–400 ng/ml), and mycophenolate mofetil (MMF) 30 mg/kg, both of which started from day −3. Cord blood (CB) graft was female and contained 6.66×10^7 nucleated cells/kg and 4.77×10^5 $CD34^+$ cells/kg. The HLA profiles of the patient and CB unit were as follows: patient HLA A*24:02 *02:01, B*35:01 *56:01, DRB1*04:10 *09:01, and CB HLA A*24:02 *02:01, B*35:01 *40:01, DRB1*04:03 *09:01, which means mutual HLA 1 antigen mismatch in B locus. The clinical course of the patient is shown in Fig. 1. Hematopoietic engraftment was rapidly achieved, with absolute neutrophil count $>0.5 \times 10^9$/l on day 15 and platelet count $>50 \times 10^9$/l on day 29. On day 17, complete donor chimerism was confirmed in both $CD3^+$ and myeloid fractions of peripheral blood (PB) using informative short tandem repeat-PCR technique. The patient started having spiking fever >39 °C on day 7, which was considered as pre-engraftment immune reaction (PIR) [3]. Prednisolone was started at a dose of 5 mg/day on day 9 and increased to 10 mg/day on day 12. On day 12, the patient developed acute cutaneous GVHD (stage 1), which subsided a few days later without the need for any additional treatment. Foscarnet (FCN) 80 mg/kg/day was also started on day 8 as the prophylaxis of CMV or human herpes virus 6 (HHV6) infection. The fever subsided by day 20, but reappeared on day 32. CMV pp65 antigenemia, which was monitored weekly, continued to be negative from day −4 to day 87. Reactivation status for CMV, HHV6, adenovirus (ADV), and BK virus (BKV) was also monitored weekly using real-time PCR analysis of plasma samples. No viral reactivation was observed, except for a positive result for CMV (7.7×10^7 copy/μg DNA) on day 42.

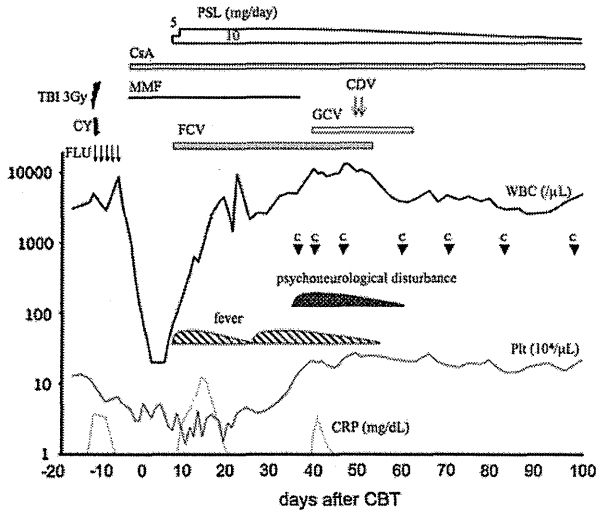

Fig. 1 Clinical course. *Bold*, *thin*, and *dotted lines* denote white blood cells (WBC) (/μL), platelets (10^4/μL), and CRP (mg/dL), respectively. *Flu* fludarabine, *CsA* cyclosporine, *MMF* mycophenolate mofetil, *PSL* prednisolone, *CY* cyclophosphamide, *TBI* total body irradiation, *FCN* foscarnet, *GCV* ganciclovir, *CDV* cidofovir, *C* CSF sample analysis

On the night of day 37, the patient's behavior suddenly became abnormal, such as cutting the infusion line with a pair of scissors or urinating on the bed board. Next morning, the patient was barely able to make even a simple conversation and his consciousness level was decreased, with the occurrence of general convulsion for a few minutes. An analysis of CSF sample on day 38 revealed that the cell number was 3464/3 μl (normal range 0–15/3 μl) consisting of polymorphonuclear leukocytes (PMN) 83 % and mononuclear cells (NMC) 17 %. The biochemical data of the CSF sample were: protein 261 mg/dl (normal range 40–75 mg/dl), Cl 116 mmol/l (normal range 120–130 mmol/l), and LDH 95 U/l (normal range 8–50 U/l). These results suggested that the patient had bacterial meningitis, but no bacterium was cultured in the CSF sample. MRI of the brain on day 39 showed no abnormal findings. Meropenem 3 g/day and ganciclovir (GCV) 3 mg/kg/day were started, with the administration of an increased dose of immunoglobulin. Real-time PCR data revealed that the CSF sample on day 38 was positive for CMV and negative for HHV6, while the PB sample was negative for the 2 viruses. There was no sign of CMV disease in other organs [4]. Follow-up data of the CSF are shown in Table 1. The CSF cell components turned to an MNC-dominant status after day 42. Although the reason why PMN was dominant in the CSF sample on day 38 is unknown, we speculate that PMN might have reflected a hyperacute inflammatory response in the central nervous system (CNS). Cidofovir 1 mg/kg/day was administered on days 50 and 52, and discontinued due to the elevation of serum creatinine level. His psychological and neurological symptoms gradually improved and completely disappeared on day 60. Follow-up brain MRI showed also normal results. He was discharged without any sequelae on day 104.

We performed the immunological characterization of CSF cells. The CSF cells on day 61 were of 100 % donor (CB) origin on chimerism analysis using STR-PCR. MNCs in the CSF mainly consisted of T cells: $CD3^+$ $CD4^+$ T cells 48.2 % and $CD3^+$ $CD8^+$ T cells 23.7 %, NK cells ($NKp46^+$ cells) 21.4 %, and B cells 0.8 %. The patient and CB shared HLA A*24:02 and A*02:01. We tested the presence of CMV-specific CD8 T cells in the PB and CSF samples on day 70 using CMV-specific HLA A*24:02-restricted and HLA A*02:01-restricted dextramers (Immudex, Copenhagen, Denmark). Dextramer staining was performed according to the manufacturer's protocol. Cells were stained with phycoerythrin-Cy7-conjugated anti-CD8, phycoerythrin-Cy5-conjugated anti-CD3 (Beckman Coulter Inc., Fullerton, CA, USA), and phycoerythrin- conjugated dextrameric-HLA A*02:01-restricted NLVPMVATV peptide complex or fluorescein isothiocyanate-conjugated

Table 1 Laboratory and viral PCR data of the CSF

Post CBT day	38	42	49	61	70	84	98
Cell number (/3 μl)	3464	1136	1336	861	376	277	217
PMN/MNC (%)	83/17	2/98	4/96	0/100	1/99	0/100	1/99
Protein (mg/dl)	261	268	289	118	107	100	96
CMV in CP CSF (copy/μg DNA)	2.8×10^6	7.5×10^5	2.0×10^4	1.6×10^2	NT	–	–
CMV in whole CSF (copy/ml)	2.8×10^6	4.9×10^7	9.1×10^5	6.7×10^2	NT	–	–
HHV6 in CP CSF (copying DNA)	–	–	–	–	NT	–	–
HHV6 in whole CSF (copy/ml)	–	–	–	–	NT	–	–
ADV in whole CSF (copy/ml)	–	–	–	–	NT	–	–
BKV in whole CSF (copy/ml)	–	–	–	–	NT	–	–

The amount of DNA of viruses, including CMV, HHV6, ADV, and BKV, in the whole or centrifuged pellet (CP) samples of the CSF was measured using real-time PCR. There was no PCR data on day 70 because most of the CSF sample was used for the flow cytometry and dextramer assay

PMN polymorphonuclear cells, *MNC* mononuclear cells, *CMV* cytomegalovirus, *HHV6* human herpes virus 6, *ADV* adenovirus, *BKV* BK virus, *NT* not tested

dextrameric-HLA A*24:02-restricted QYDPVAALF peptide complex (Immudex, Copenhagen, Denmark). After lysing red blood cells and washing twice with bovine serum albumin containing phosphate-buffered saline, cells were examined on a flow cytometer (Cytomics FC 500, Beckman Coulter, Inc., USA). More than 100,000 cells were acquired in the lymphocyte gate and analyzed using CXP software. The percentage of CMV-specific dextramer-positive cells in the $CD3^+$ $CD8^+$ fraction is shown in Table 2. The dextramer-negative control value in the CSF was a little high; however, these data suggest that the percentage of CMV-specific T cells is higher in the CSF than in the PB at least for A*02:01 dextramer. CMV-specific CD8 T cells seemed to be dominantly HLA A*02:01-restricted, but direct comparison was limited due to the difference in the efficacy of the two dextramers. Of note, CSF cell numbers were maintained still at high levels even after CMV DNA became undetectable (Table 1).

Table 2 CMV-specific T cells (%) in the $CD3^+$ $CD8^+$ fraction

	A*02:01 dextramer	A*24:02 dextramer	Dextramer (−)
PB	0.01	0.26	0.01
CSF	1.19	0.47	0.19

Discussion

Cytomegalovirus disease of the CNS is a rare complication after allogeneic SCT in patients. Reddy et al. [4] recently summarized 11 cases of CMV disease of the CNS after SCT. According to their report, all cases developed CMV CNS disease at late onset (occurring 166 or more days after transplantation), were ganciclovir resistant, and ten of them expired despite antiviral combination therapy. Drug resistance was pointed out to be a key factor in the occurrence of CMV CNS disease [5]. In our case, the CMV disease was also suggested to be relatively FCN resistant, since CMV-ME developed during prophylactic FCN administration. In accordance with the previous report [4], there was no evidence of CMV disease in organs other than CNS. The patient did not even show CMV antigenemia or positive PCR test for CMV DNA using the plasma samples except for one (PCR data on day 42). The occurrence of CMV CNS lesion in an isolated form may reflect a relatively low penetration of FCN, as described by Reddy et al. CMV disease of the CNS is reported to develop at late onset because drug resistant virus appears after a relatively long period of drug therapy. On the other hand, CMV-ME in our case that developed in a form as related to PIR in the engraftment period is similar to post-transplant HHV-6 encephalitis, which was reported to develop in association with the production of inflammatory cytokines such as interleukin-6 [6]. Furthermore, in our case, the absence of abnormal findings of MRI of the brain may have resulted in complete recovery of this serious complication.

There have been no reports showing the presence of CMV-specific CTLs in the CFS of patients with CMV-ME. Regarding the detection of virus-specific CTLs in the CSF, JC virus-specific CTLs in patients with progressive multifocal leukoencephalopathy [7], and HIV-specific $CD8^+$ T cells in antiretroviral therapy-naïve HIV-positive subjects [8], have been reported. These studies suggest that the presence of virus-specific CTLs in the CSF has a beneficial effect in controlling these viral CNS diseases. Likewise, the presence of CMV-specific CTLs in the CSF in our case may have exerted some beneficial effects, although ganciclovir and/or cidofovir are considered to have contributed to controlling CMV-ME. In the present report, we first showed the existence of CMV-specific T cells in CSF samples of the patient with CMV-ME. In addition, we

underlined that CMV-specific T cells were of donor origin (CB derived), and that the frequency of CMV-specific T cells was higher in CSF than in PB. In macaques, activated T cells were reported to preferentially enter the intrathecal compartment and increase in frequency early after acute simian immunodeficiency virus infection [9]. Furthermore, rodent data suggest that the expression of viral antigens in the brain may upregulate endothelial cell major histocompatibility complex class I expression, contributing to $CD8^+$ T cell migration into the brain [10]. Taken together with these findings, we consider in our case that CB-derived CMV-specific T cells may develop early in transplantation and enter the intrathecal compartment.

Acknowledgments We thank the medical, nursing, and laboratory staff of the participating departments for their contributions. We are also grateful to Ms. Aya Yano and Ms. Kimiko Yamamoto for their excellent technical assistance.

Conflict of interest The authors declare no competing financial interests.

References

1. Schmidt-Hieber M, Schwender J, Heinz WJ, Zabelina T, Kühl JS, Mousset S, et al. Viral encephalitis after allogeneic stem cell transplantation: a rare complication with distinct characteristics of different causative agents. Haematologica. 2011;96:142–9.
2. Misawa M, Kai S, Okada M, Nakajima T, Nomura K, Wakae T, et al. Reduced-intensity conditioning followed by unrelated umbilical cord blood transplantation for advanced hematologic malignancies: rapid engraftment in bone marrow. Int J Hematol. 2006;83:74–9.
3. Kishi Y, Kami M, Miyakoshi S, Kanda Y, Murashige N, Teshima, et al. Early immune reaction after reduced-intensity cord-blood transplantation for adult patients. Transplantation. 2005;80:34–40.
4. Reddy SM, Winston DJ, Territo MC, Schiller GJ. CMV central nervous system disease in stem-cell transplant recipients: an increasing complication of drug-resistant CMV infection and protracted immunodeficiency. Bone Marrow Transplant. 2010; 45:979–84.
5. Julin JE, van Burik JH, Krivit W, Webb C, Holman CJ, Clark HB, et al. Ganciclovir-resistant cytomegalovirus encephalitis in a bone marrow transplant recipient. Transpl Infect Dis. 2002;4:201–6.
6. Ogata M, Satou T, Kawano R, Takakura S, Goto K, Ikewaki J, et al. Correlations of HHV-6 viral load and plasma IL-6 concentration with HHV-6 encephalitis in allogeneic stem cell transplant recipients. Bone Marrow Transplant. 2010;45:129–36.
7. Du Pasquier RA, Autissier P, Zheng Y, Jean-Jacques J, Koralnik IJ. Presence of JC virus-specific CTL in the cerebrospinal fluid of PML patients: rationale for immune-based therapeutic strategies. AIDS. 2005;19:2069–76.
8. Sadagopal S, Lorey SL, Barnett L, Basham R, Lebo L, Erdem H, et al. Enhancement of human immunodeficiency virus (HIV)-specific CD8+ T cells in cerebrospinal fluid compared to those in blood among antiretroviral therapy-naive HIV-positive subjects. J Virol. 2008;82:10418–28.
9. Kim WK, Corey S, Chesney G, Knight H, Klumpp S, Wüthrich C, et al. Identification of T lymphocytes in simian immunodeficiency virus encephalitis: distribution of CD8+ T cells in association with central nervous system vessels and virus. J Neurovirol. 2004;10:315–25.
10. Galea I, Bernardes-Silva M, Forse PA, van Rooijen N, Liblau RS, Perry VH. An antigen-specific pathway for CD8 T cells across the blood–brain barrier. J Exp Med. 2007;204:2023–30.